

## Imaging Lysosomal pH Alteration in Stressed Cells with a Sensitive Ratiometric Fluorescence Sensor

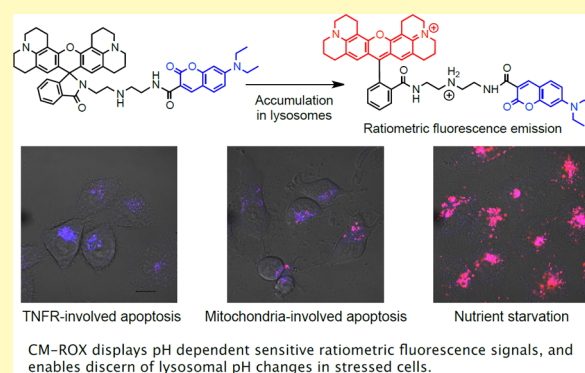
Zhongwei Xue,<sup>†,‡,§,||,⊥,¶,♯</sup> Hu Zhao,<sup>†,‡,§,||,⊥,¶,♯</sup> Jian Liu,<sup>†,‡,§,||,⊥,¶</sup> Jiahuai Han,<sup>¶,▽,■</sup> and Shoufa Han<sup>\*,†,‡,§,||,⊥,¶</sup>

<sup>†</sup>Department of Chemical Biology, <sup>‡</sup>College of Chemistry and Chemical Engineering, <sup>§</sup>State Key Laboratory for Physical Chemistry of Solid Surfaces, <sup>||</sup>The Key Laboratory for Chemical Biology of Fujian Province, <sup>⊥</sup>The MOE Key Laboratory of Spectrochemical Analysis & Instrumentation, <sup>¶</sup>Innovation Center for Cell Signaling Network, <sup>▽</sup>State Key Laboratory of Cellular Stress Biology, and <sup>■</sup>School of Life Sciences, Xiamen University, Xiamen, 361005, China

## Supporting Information

**ABSTRACT:** The organelle-specific pH is crucial for cell homeostasis. Aberrant pH of lysosomes has been manifested in myriad diseases. To probe lysosome responses to cell stress, we herein report the detection of lysosomal pH changes with a dual colored probe (CM-ROX), featuring a coumarin domain with “always-on” blue fluorescence and a rhodamine–lactam domain activatable to lysosomal acidity to give red fluorescence. With sensitive ratiometric signals upon subtle pH changes, CM-ROX enables discernment of lysosomal pH changes in cells undergoing autophagy, cell death, and viral infection.

**KEYWORDS:** lysosome, pH changes, ratiometric fluorescence imaging, autophagy, cell death, viral infection



The organelle-specific pH, critical for cell homeostasis, is elaborately controlled and yet succumbs to pathological inducers. Lysosomes are the major intracellular acidic compartments, and the lysosomal acidity is critical for diverse biological events ranging from autophagy, cell death, to immunity.<sup>1</sup> Aberrant lysosomal pH is manifested in myriad diseases. For instance, lysosomes could be acidified in immune cell maturation and inflammation, whereas chronically elevated lysosomal pH occurs in aging and lysosomal storage diseases.<sup>2</sup> As such, defining lysosomal pH changes mediated by pathological inducers would be of use to decipher the roles of lysosomes in diseases.

Ratiometric fluorescence imaging enables enhanced accuracy by normalizing uncertainties associated with single intensity fluorophores, e.g., uneven probe distribution. Hence, dual emissive nanoparticles have been widely employed for intracellular pH imaging.<sup>3</sup> Individual lysosomes are of distinct pH and sub-cellular locations. Apart from the liability to be distributed at extra-lysosomal settings, e.g., cytosol, nanoprobe are individually endocytosized into discrete lysosomes, leading to staining of a fraction of lysosomes. As such, lysosome-homing molecular probes that are trapped in lysosomes via passive diffusion are advantageous to study global lysosome responses in cells. Complementing de novo design of single fluorophores displaying pH dependent dual emission bands,<sup>4</sup> integration of existing fluorophores provides an alternative approach for ratiometric imaging of lysosomes.<sup>5</sup>

We recently reported ratiometric imaging of mitochondrial depolarization with triphenylphosphonium-conjugated ROX-lactam/coumarin (RC-TPP), which accumulates in mitochondria of alkaline lumen to give blue fluorescence, and relocates into acidic lysosomes to give rhodamine fluorescence.<sup>6</sup> Herein we report the derivatization and integration of coumarin and rhodamine, two classic fluorophores of exceptional photophysical properties, to yield a self-referenced pH sensor with highly advantageous optical properties for imaging lysosomal acidity. The chimeric probe (CM-ROX) features a coumarin moiety displaying “always-on” blue fluorescence, rhodamine-X-lactam moiety (ROX) of red fluorescence activatable to acidic lysosomes, and an acidotropic diethylenetriamine linker. CM-ROX is compatible to Green Fluorescent Protein imaging and displays a strong ratiometric response to subtle pH changes. These advantageous properties of CM-ROX enable discernment of lysosomal pH changes in cells undergoing autophagy, cell death, and viral infection. Using the same pH reporting entities as mitochondria-targeting RC-TPP,<sup>6</sup> the capability of CM-ROX to image lysosomes over mitochondria evidences the utility of ratiometric sensors integrated with appropriate organelle-specific linkers to probe novel biology of distinct organelles.

Received: January 17, 2017

Accepted: February 27, 2017

Published: February 27, 2017

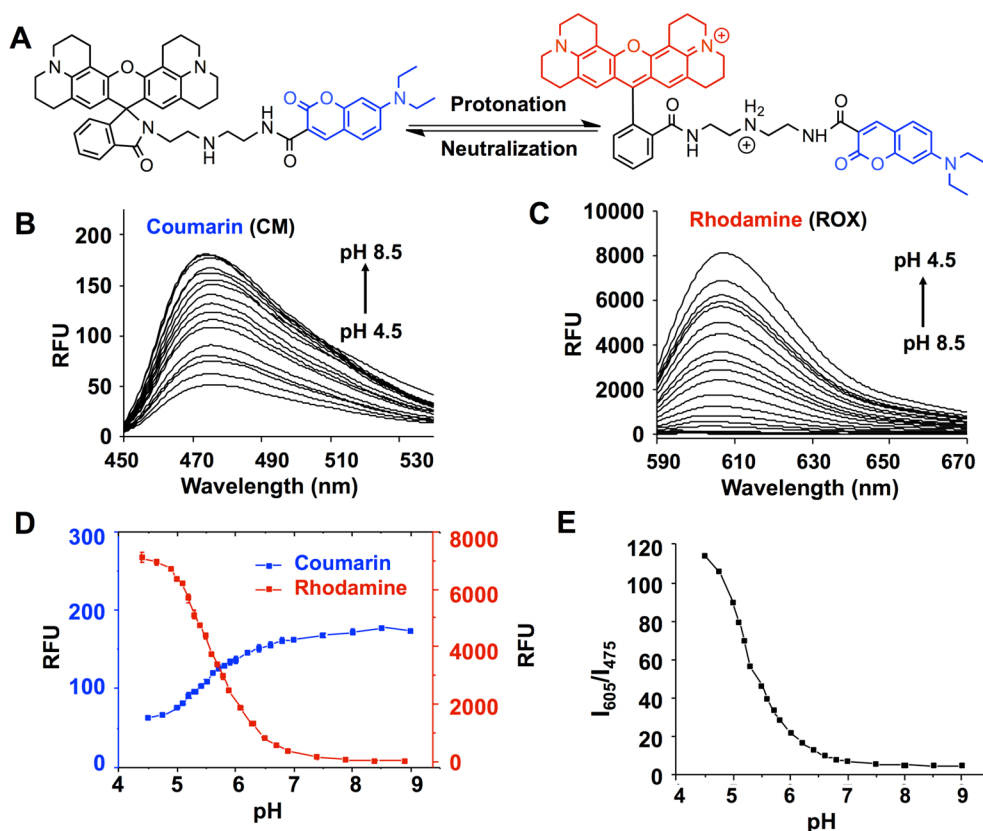


**Figure 1.** pH mediated ratiometric fluorescence of CM-ROX. (A) Proton triggered isomerization of CM-ROX gives rhodamine fluorescence. (B) Coumarin fluorescence emission of CM-ROX ( $5 \mu\text{M}$ ) at pH 4.5–8.5 ( $\lambda_{\text{ex}} = 435 \text{ nm}$ ). (C) Rhodamine fluorescence emission of CM-ROX ( $5 \mu\text{M}$ ) at pH 4.5–8.5 ( $\lambda_{\text{ex}} = 590 \text{ nm}$ ). (D) pH titration curves of CM-ROX; fluorescence emission intensity of rhodamine ( $\lambda_{\text{em}} = 605 \text{ nm}$ ) and that of coumarin ( $\lambda_{\text{em}} = 475 \text{ nm}$ ) were respectively plotted over buffer pH. (E) pH dependent ratios of rhodamine fluorescence ( $I_{605}$ ) to that of coumarin fluorescence ( $I_{475}$ ).

## EXPERIMENTAL SECTION

BFA was purchased from Selleck. Rapamycin, CCCP, TNF, and Smac mimetic were obtained from Sigma. CM-ROX was synthesized as reported.<sup>6</sup> All other chemicals were obtained from Alfa-Aesar. Cell lines were obtained from American Type Culture Collection. Lentiviral infection was used for stable expression. Recombinant lentiviruses were packaged in 293T cells in the presence of helper plasmids (pMDLg, pRSV-REWV, and pVSV-G). Cells were maintained in Dulbecco's modified Eagle's medium (DMEM) with 10% fetal bovine serum, 2 mM L-glutamine, 100 IU penicillin, and 100 mg/mL streptomycin. Full-length cDNA of Lamp2 were cloned using the method as described.<sup>7</sup> Fluorescence analysis was performed on SpectraMax M5. Confocal microscopic imaging was performed on Zeiss LSM 780 using  $\lambda_{\text{ex}} = 405 \text{ nm}$  and  $\lambda_{\text{em}} = 410\text{--}490 \text{ nm}$  for coumarin,  $\lambda_{\text{ex}} = 488 \text{ nm}$  and  $\lambda_{\text{em}} = 490\text{--}553 \text{ nm}$  for GFP,  $\lambda_{\text{ex}} = 565 \text{ nm}$  and  $\lambda_{\text{em}} = 593\text{--}735 \text{ nm}$  for rhodamine. Signals of rhodamine and coumarin in cells were respectively shown in red and blue, while GFP was shown in green. Images were merged using Photoshop CS6. Quantitative analysis was carried out on unprocessed images using ImageJ software. The graph was generated by GraphPad Prism5 and origin 8.0 software.

**pH Titration of CM-ROX.** CM-ROX was added to Tris-HCl buffer containing 40% MeOH (pH: 4.5, 4.75, 5.0, 5.1, 5.2, 5.3, 5.4, 5.5, 5.6, 5.7, 5.8, 5.9, 6.2, 6.4, 6.6, 6.8, 7.0, 7.5, 8.0, 8.5) to a final concentration of  $5 \mu\text{M}$ . Fluorescence spectra were recorded using  $\lambda_{\text{ex}} = 425 \text{ nm}$  for CM and  $\lambda_{\text{ex}} = 590 \text{ nm}$  for ROX.

**Imaging of Lysosomes with CM-ROX.** Lam2-GFP<sup>+</sup> HeLa cells were incubated in DMEM supplemented with CM-ROX ( $2 \mu\text{M}$ ) for 30 min, further incubated in DMEM spiked with or without BFA (40 nM) for 4 h, and then analyzed by confocal fluorescence microscopy and flow cytometry. 10 000 cells were gated under identical

conditions whereby coumarin fluorescence was recorded by FL1 filter ( $\lambda_{\text{em}}: 430\text{--}470 \text{ nm}$ ;  $\lambda_{\text{ex}}: 405 \text{ nm}$ ) while that of ROX was recorded by FL2 filter ( $\lambda_{\text{em}}: 590\text{--}630 \text{ nm}$ ;  $\lambda_{\text{ex}}: 561 \text{ nm}$ ). In parallel, HeLa, L929, CHO, and MCF-7 cells were incubated in DMEM containing CM-ROX ( $2 \mu\text{M}$ ) before analysis by confocal fluorescence microscopy and flow cytometry. For confocal microscopic analysis, 10 lysosomes from 5 cells selected randomly were analyzed. The ratio of channel 1 (coumarin,  $\lambda_{\text{em}} = 410\text{--}490 \text{ nm}$ ) to channel 2 (rhodamine,  $\lambda_{\text{em}} = 593\text{--}735 \text{ nm}$ ) was calculated using the value of selected lysosomes given by the ImageJ software. For average lysosomal acidity, 5 cells were randomly selected where the pH of 10 lysosomes were determined and averaged.

**Detecting Changes of Lysosomal Acidity in Autophagy and Apoptosis.** For autophagy: HeLa cells were cultured in DMEM spiked with CM-ROX ( $2 \mu\text{M}$ ) for 30 min, further cultivated in HBSS, HBSS containing BFA, DMEM, or DMEM spiked with CCCP ( $20 \mu\text{M}$ ), BFA (40 nM), or rapamycin ( $10 \mu\text{M}$ ) for 2 h. For apoptosis: HeLa cells were cultured in DMEM containing CM-ROX ( $2 \mu\text{M}$ ) for 30 min and then further cultured for 2 h in DMEM spiked with no addition, STS ( $2 \mu\text{M}$ ), or TNF ( $20 \text{ ng/mL}$ ) and Smac mimetic ( $100 \text{ nM}$ ). These cells were analyzed by confocal fluorescence microscopy and flow cytometry.

**Imaging of Lysosomal pH Changes in Cells Infected by HSV-1 and VSV.** HeLa cells were cultured in DMEM spiked with CM-ROX ( $2 \mu\text{M}$ ) for 30 min and then further incubated in DMEM containing type I Herpes Simplex Virus-1 ( $10^5 \text{ MOI}$ ), Vesicular Stomatitis Virus ( $1.5 \times 10^4 \text{ MOI}$ ) or no addition for 0–3 h. Then cells were analyzed by confocal microscopy.

**Cytotoxicity of CM-ROX.** The cytotoxicity of CM-ROX was evaluated on HeLa cells. The cells were cultured with medium containing CM-ROX (0, 1, 2, 5, and  $10 \mu\text{M}$ ) for 30 min and washed with DMEM for 3 times then incubated with fresh medium for 6, 12,

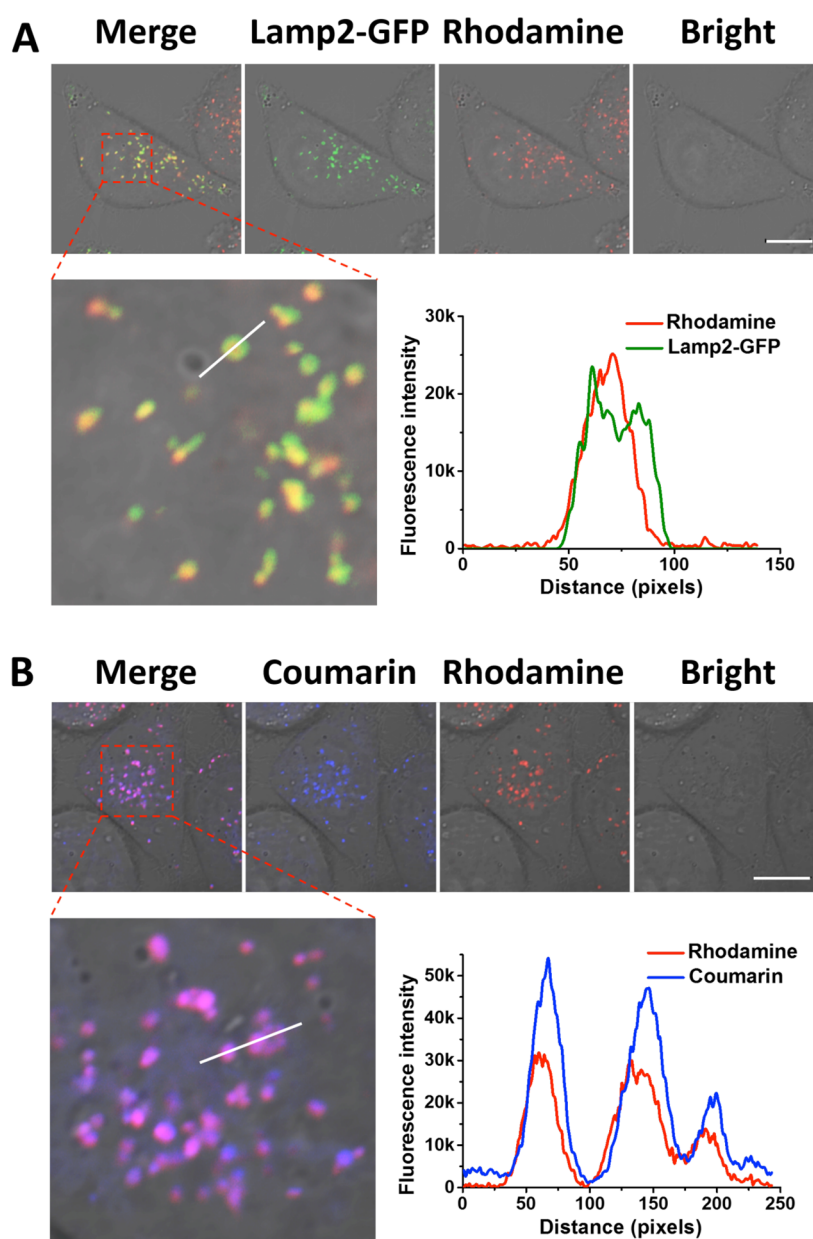


**Figure 2.** Dual colored lysosome imaging with CM-ROX. Lamp2-GFP<sup>+</sup> HeLa cells were stained with CM-ROX (3  $\mu$ M) for 30 min and then visualized by confocal fluorescence microscopy for colocalized fluorescence of rhodamine with GFP (A) and coumarin (B). Scans taken through the indicated line reveal fluorescence colocalization of rhodamine with coumarin, and Lamp2-GFP. Bar, 10  $\mu$ m.

24, and 48 h. The cell number and cell viability were determined by MTS assay.

**Photostability of CM-ROX.** HeLa cells were incubated with CM-ROX (2  $\mu$ M), LysoTracker Blue (2  $\mu$ M), or LysoTracker Red (2  $\mu$ M) for 30 min at 37  $^{\circ}$ C under 5% CO<sub>2</sub> in DMEM supplemented with 10% fetal bovine serum. The culturing media were removed and replaced with fresh medium for 3 times. Then cells were scanned 10 times with a confocal fluorescence microscope ( $\lambda_{\text{ex}}$  = 405 nm for CM and LysoTracker Blue,  $\lambda_{\text{ex}}$  = 561 nm for ROX and LysoTracker Red). The images were analyzed using ImageJ software.

## RESULTS AND DISCUSSION

Rhodamine-lactams are a group of nonfluorescent rhodamine derivatives prone to proton mediated fluorogenic opening of intramolecular lactams, allowing “signal-on” lysosome imaging.<sup>6,8</sup> We recently reported optical tracking of phagocytosis using ROX-lactam labeled bacteria.<sup>9</sup> Highly sensitive to acidic

pH and with photophysical properties complementing Green Fluorescent Protein (GFP) technology, ROX-lactam was hence bridged with coumarin via diethylenetriamine linker to enable protonation mediated lysosomal accumulation and ensuing reporting of lysosome pH variations in stressed cells (Figure 1A).

**pH Mediated Ratiometric Responses of CM-ROX.** pH titration of CM-ROX shows rhodamine fluorescence peaked at 605 nm, was negligible at pH 7.0–8.5, occurred in acidic media, and intensified as pH decreases (pH 6.5–4.5) (Figure 1B) with calculated  $pK_a$  of 5.69 (Figure S7, Supporting Information), which is consistent with proton mediated fluorogenic opening of the intramolecular lactam (Figure 1A). Concomitant with dramatically increased rhodamine signal at acidic pH, CM-ROX displays coumarin fluorescence moderately declining as pH decreases (Figure 1B,C). The reversed pH responses of rhodamine over coumarin enable imaging of subtle acidification

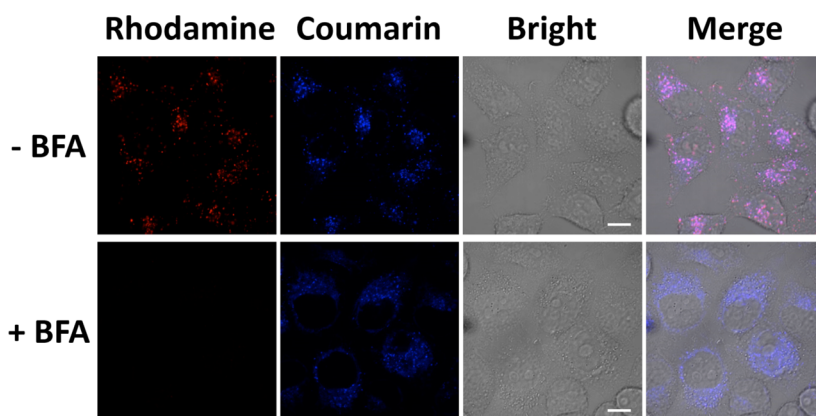


**Figure 3.** Lysosomal acidity-dependent activation of ROX-lactam. HeLa cells were cultivated in DMEM spiked with or without BFA (40 nM) for 4 h and then stained with CM-ROX (2  $\mu$ M) for 30 min before confocal microscopy analysis. Bar, 10  $\mu$ m.

in the range of pH 6.0–4.5 by pronounced changes in ratios of fluorescence intensity (Figure 1D,E). For instance,  $I_{605\text{ nm}}/I_{485\text{ nm}}$  interval between pH 4.5 and pH 5.5 was 70, whereas commercial lysosensors often exhibited moderate ratio changes (around 0.3) per pH unit (Figure 1D).<sup>10</sup> Overlay of the optimal sensing range of CM-ROX (pH 6.0–4.5) with lysosome acidity window (pH 6.0–4.5) indicates the applicability of CM-ROX to monitor lysosomal pH changes.

**Lysosome-Specific Ratiometric Fluorescence of CM-ROX.** We then pulsed CM-ROX with HeLa cells expressing Lamp2-GFP (GFP-tagged lysosome associated membrane protein-2). Punctate rhodamine signals stringently eclipse GFP and coumarin fluorescence inside cells (Figure 2). As Lamp2 is a constitutive protein marker of lysosomes, these results clearly show that CM-ROX effectively accumulates in lysosomes to give rhodamine signals, and demonstrate the compatibility of CM-ROX ( $\lambda_{\text{em}}$ : 605/475 nm) with GFP ( $\lambda_{\text{em}}$ : 510 nm) for three colored cell images. The demonstrated accumulation of CM-ROX in lysosomes is ascribed to protonation of the diethylenetriamine linker and protonation of ROX-lactam moiety in acidic lysosomes (Figure 1A). To confirm acidity dependent probe activation in lysosomes, HeLa cells were costained with CM-ROX and Bafilomycin A1 (BFA), which is an ATP-H1 pump inhibitor and is able to neutralize lysosomal pH.<sup>11</sup> Rhodamine fluorescence, present in BFA-free control cells, vanished in BFA treated cells (Figure 3), proving lysosomal acidity mediated activation of CM-ROX inside cells.

The cytotoxicity of CM-ROX was evaluated in HeLa cells by MTS assay. No toxic effects were observed on cell viability after incubation with CM-ROX at doses up to 10  $\mu$ M (Supporting Information, Figure S1), which was 5-fold higher than the concentration used in lysosomal imaging. In addition, HeLa cells precultured with CM-ROX or commercial dyes specific for lysosomes were respectively exposed to multiple laser illumination, and the intracellular fluorescence intensity was recorded over illumination times by fluorescence microscopy. CM-ROX exhibited constant red fluorescence in lysosomes comparable to LysoTracker Red and stable blue fluorescence whereas the fluorescence of LysoTracker blue quickly decayed upon laser illumination (Supporting Information, Figure S2). The superior photostability and low cytotoxicity of CM-ROX facilitates its applicability for long-term optical tracking of lysosomal changes in live cells.

**Imaging of Cell Line-Specific Lysosomal pH.** CM-ROX was further assessed to differentiate lysosomes of L929, HeLa,

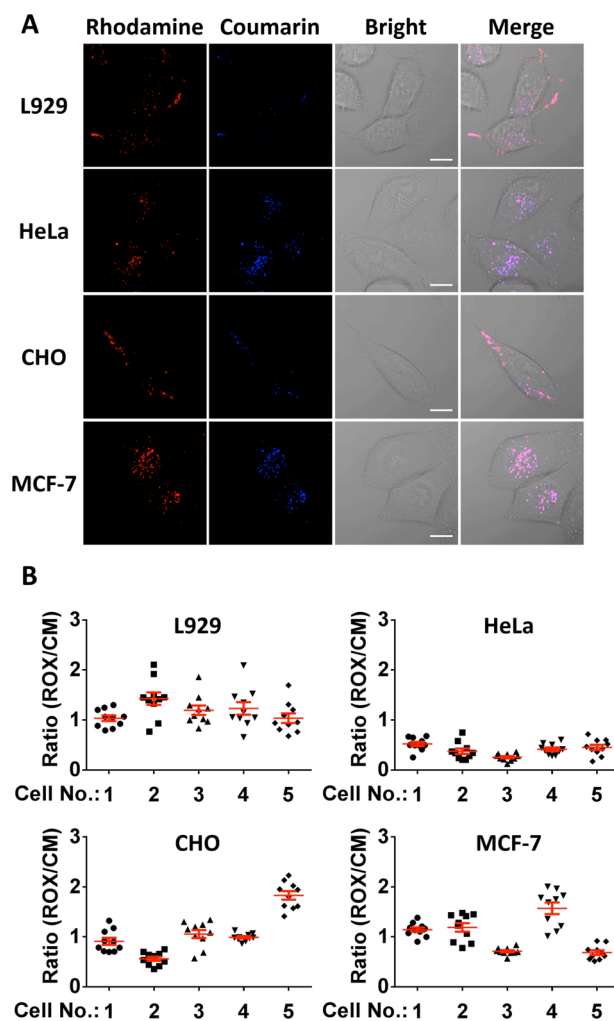


**Figure 4.** Imaging of cell line-specific lysosomal pH with CM-ROX by confocal fluorescence microscopy. HeLa, L929, CHO, and MCF-7 cells were cultivated in DMEM supplemented with CM-ROX (2  $\mu$ M) for 30 min and then visualized by confocal fluorescence microscopy (A). For each type of cells, 10 individual lysosomes of 5 cells were analyzed for  $I_{\text{ROX}}/I_{\text{CM}}$  (B). Bar, 10  $\mu$ m.

CHO, and MCF-7 cells. Dual colored emission of CM-ROX was clearly observed in all cell lines examined. Ratios of fluorescence emission intensity of ROX to CM ( $I_{\text{ROX}}/I_{\text{CM}}$ ) was measured and used as the indicator of lysosomal pH.

Quantitative analysis of 10 lysosomes from 5 cells showed that lysosomes within the same cell are of distinct pH values, and the mean lysosomal pH is cell-type dependent (Figure 4). For instance, lysosomal pH in HeLa cells is significantly less acidic relative to L929, CHO, and MCF-7 cells. Moreover, the distinct global lysosomal pH patterns revealed by flow cytometry in these cell lines are consistent with the patterns observed by confocal microscopic analysis (Figure S3, Supporting Information). These results show the applicability of CM-ROX to differentiate pH of individual lysosomes or total lysosomes in cell populations.

#### Imaging of Lysosomal pH Changes in Autophagy.

Autophagy is a conserved process mediating degradation of dysfunctional cellular components in response to diverse stress cues, such as starvation. Insufficient autophagy has been linked to Parkinson's disease and chronic infection.<sup>12</sup> Shown to discern lysosomes pH in resting cells, CM-ROX was further evaluated to monitor lysosomal pH changes triggered by starvation and autophagic inducers of rotenone, rapamycin, and carbonyl cyanide *m*-chlorophenylhydrazone (CCCP).<sup>13</sup> Cells cultivated in Hanks' balanced salt solution (HBSS) display dramatically enhanced ratios of rhodamine to coumarin, showing lysosomal acidification upon starvation, whereas cells treated with rotenone, rapamycin, or CCCP display attenuated  $I_{\text{ROX}}/I_{\text{CM}}$  indicative of moderate elevation of lysosomal pH. Dramatically suppressed rhodamine signals and  $I_{\text{ROX}}/I_{\text{CM}}$  were observed in HBSS-treated cell in the presence of BFA (Figure 5), which effectively neutralizes lysosomes, proving starvation mediated lysosomal acidification. Previous studies

using monoemissive lysotrackers suggest lysosomal acidification in starved cells.<sup>14</sup> Apart from lysosomal pH, intracellular fluorescence could also be affected by the number of lysosomes. Overcoming limitations of monoemissive dyes, our approach employs pH mediated ratiometric fluorescence of CM-ROX to unambiguously delineate lysosomal pH changes in autophagic cells.

#### Discerning Lysosomal pH Changes in Apoptotic Cells.

As an important cell death modality, apoptosis occurs under physiological conditions and is required for cell and tissue homeostasis.<sup>15</sup> Apoptosis could be executed in distinct cell signaling events, including cell surface death receptor-triggered apoptosis, e.g., tumor necrosis factor receptor, and mitochondria mediated apoptosis featuring the release of cytochrome c from mitochondria into cytosol.<sup>16</sup> To discern lysosomes in different apoptosis routes, HeLa cells stained with CM-ROX were treated with human Tumor Necrosis Factor- $\alpha$  (TNF) and Smac, which trigger apoptosis by dimerization of cell surface TNF receptor, or treated with staurosporine (STS) to activate mitochondria-mediated apoptosis.<sup>17</sup> At 2 h post-stimulation, STS-treated cells display obviously enhanced intracellular rhodamine signals and  $I_{\text{ROX}}/I_{\text{CM}}$ , whereas negligible alteration was observed in cells treated with TNF (Figure 6), showing lysosomal acidification during STS-induced apoptosis over TNF-mediated apoptosis. These results show the capability of CM-ROX to differentiate the interplay of lysosomes with different cell death signaling events.

#### Imaging of Lysosomal pH Changes during Viral Infection.

Viruses evolve diverse mechanisms to infect host

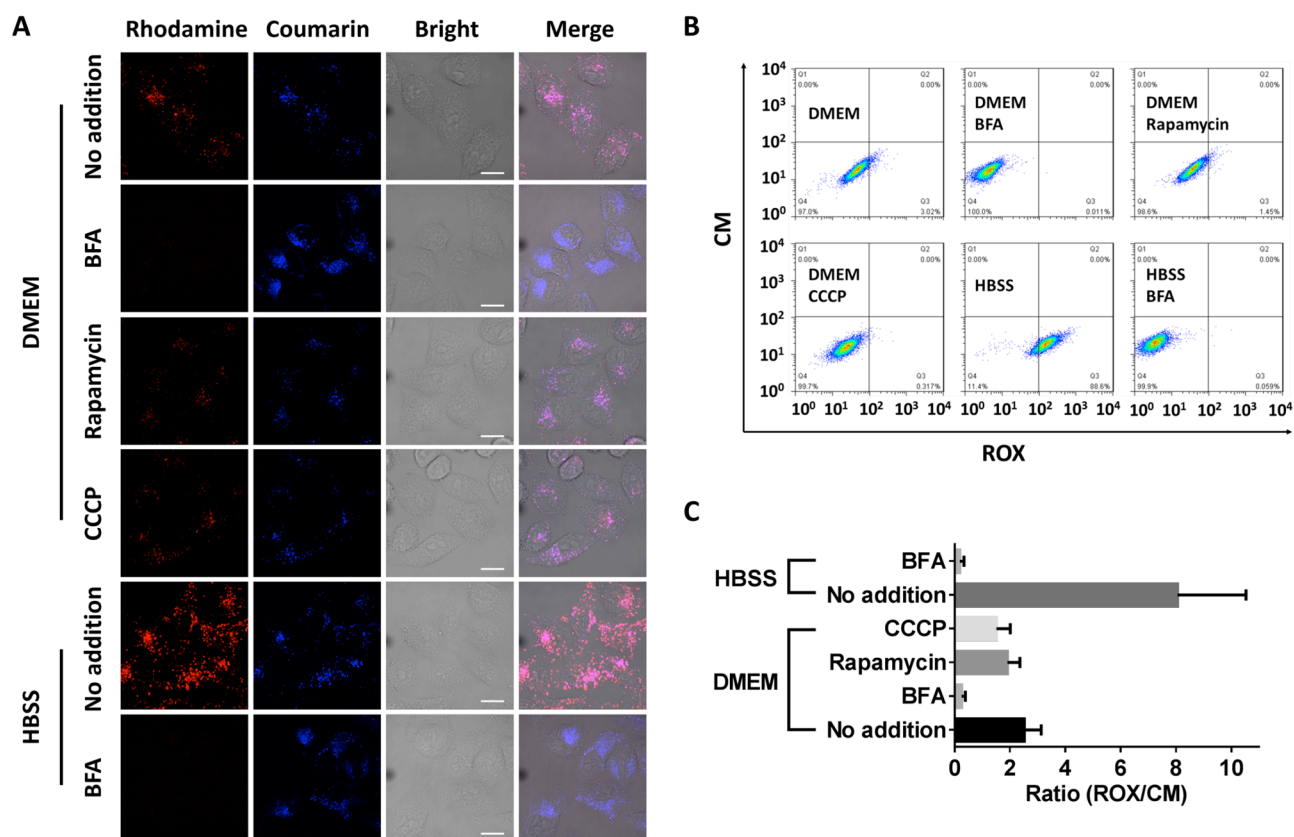


**Figure 5.** Detection of lysosomal pH changes in distinct autophagy signaling events with RC-ROX. HeLa cells prestained with CM-ROX (2  $\mu\text{M}$ ) were respectively cultivated for 2 h in HBSS spiked with or without BFA, DMEM spiked with rapamycin, DCCP, BFA, or no addition, and then analyzed by confocal fluorescence microscopy (A) or flow cytometry (B). Statistical results of  $I_{\text{ROX}}/I_{\text{CM}}$  were measured by flow cytometry (C). Bar, 10  $\mu\text{m}$ .

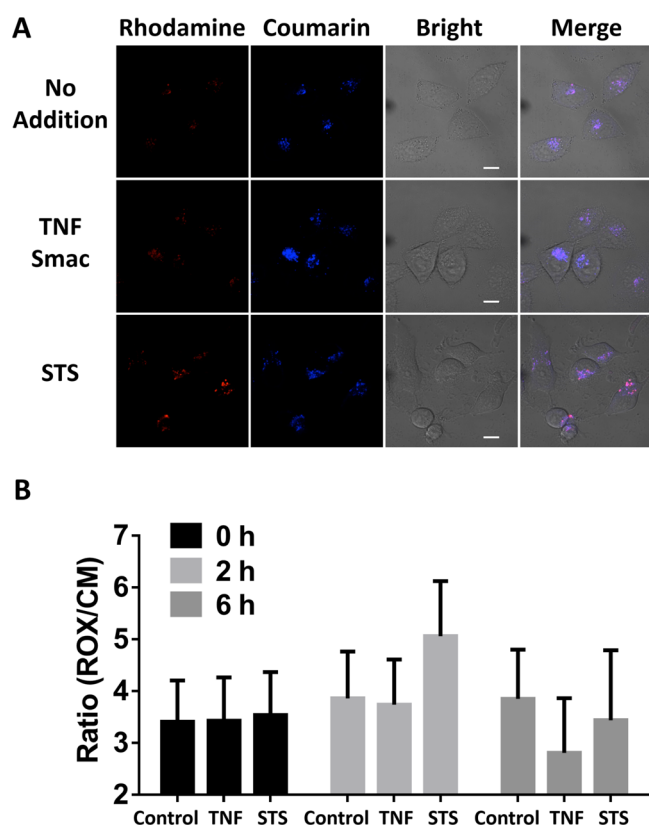


**Figure 6.** Detection of lysosomal pH alterations in distinct cell death signaling events. HeLa cells prestained with CM-ROX ( $2 \mu\text{M}$ ) were cultivated for 0–6 h in DMEM containing STS, a combination of tumor necrosis factor- $\alpha$  (TNF- $\alpha$ ) and Smac, or no addition, and then analyzed by confocal fluorescence microscopy (2 h) (A) or flow cytometry (B). Bar,  $10 \mu\text{m}$ .

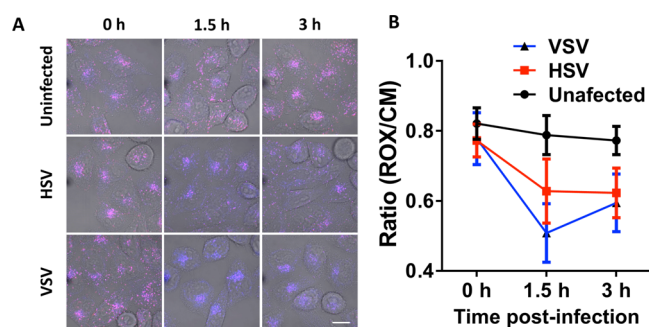


**Figure 7.** Imaging lysosome neutralization in cells infected by HSV or VSV. HeLa cells prestained with CM-ROX ( $2 \mu\text{M}$ ) were cultivated for 0–3 h in DMEM containing HSV-1, VSV, or no addition. They are then analyzed by confocal fluorescence microscopy (A) and flow cytometry for intracellular fluorescence ratios of rhodamine to coumarin (B). Bar,  $20 \mu\text{m}$ .

cells, of which viruses internalized into intracellular acidic compartments could escape lysosomes by acidic pH-induced fusion of viral membrane and lysosome membrane. For instance, Vesicular Stomatitis Virus (VSV) is an animal virus requiring lysosomes for infection.<sup>18</sup> By contrast, Herpes Simplex Virus (HSV), causing life-long infection in human, could infect cells in both pH-dependent and pH-independent routes.<sup>19</sup> Although not required, the acidic pH of endolysosomes has been shown to augment infectivity of HSV in a cell-type dependent manner.<sup>20</sup> To examine the responses of

lysosomes in viral infection, HeLa cells prestained with CM-ROX were infected with VSV or HSV-1. Time course imaging shows that intracellular rhodamine signals and  $I_{\text{ROX}}/I_{\text{CM}}$  are markedly decreased in HSV-1 and VSV-treated cells at 1.5–3 h post-infection (Figure 7, and Figure S4, Supporting Information), indicating that both viruses could effectively neutralize lysosomes in HeLa cells. The results strongly indicate the use of CM-ROX as a sensitive tool for real-time monitoring of dynamic lysosome responses triggered by viral infection.

## CONCLUSIONS

Aberrant lysosomal pH has been manifested in diverse diseases. CM-ROX, integrating acidity activatable ROX-lactam and coumarin fluorophore, was developed for sensing of lysosomal acidity in cell stress. CM-ROX displays ratiometric fluorescence signals highly sensitive to pH changes and lysosome specific accumulation in live cells, which enables tracking of lysosomal pH changes in stressed cells undergoing autophagy, cell death, and viral infection. Compared with monoemissive fluorophores, CM-ROX holds widespread implications to study the roles of dynamic lysosomes in diverse cell signaling events and disease relevant cell stress.

## ASSOCIATED CONTENT

### Supporting Information

The Supporting Information is available free of charge on the ACS Publications website at DOI: [10.1021/acssensors.7b00035](https://doi.org/10.1021/acssensors.7b00035).

Cytotoxicity and photostability of CM-ROX, flow cytometry analysis of global lysosomal pH with CM-ROX, and statistical results of time-lapsed lysosomal pH change in cells infected by HSV-1 and VSV (PDF)

## AUTHOR INFORMATION

### Corresponding Author

\*E-mail: [shoufa@xmu.edu.cn](mailto:shoufa@xmu.edu.cn). Fax: +865922181728.

### ORCID

Shoufa Han: 0000-0002-2057-0559

### Author Contributions

#Zhongwei Xue and Hu Zhao contributed equally to this work.

### Notes

The authors declare no competing financial interest.

## ACKNOWLEDGMENTS

This work was supported by grants from 973 program 2013CB933901, NSF China (21572189, 21272196), the Fundamental Research Funds for the Central Universities (20720160052, 20720150047); Dr. J. Han was supported by grants from NSF China (91429301, 31420103910, 31330047, 31221065), the National Scientific and Technological Major Project (2013ZX10002-002), the Hi-Tech Research and Development Program of China (863program; 2012AA02A201).

## REFERENCES

- (1) Kroemer, G.; Jaattela, M. Lysosomes and autophagy in cell death control. *Nat. Rev. Cancer* **2005**, *5* (11), 886–97.
- (2) (a) Di, A.; Brown, M. E.; Deriy, L. V.; Li, C.; Szeto, F. L.; Chen, Y.; Huang, P.; Tong, J.; Naren, A. P.; Bindokas, V.; Palfrey, H. C.; Nelson, D. J. CFTR regulates phagosomal acidification in macrophages and alters bactericidal activity. *Nat. Cell Biol.* **2006**, *8* (9), 933–44. (b) Trombetta, E. S.; Ebersold, M.; Garrett, W.; Pypaert, M.; Mellman, I. Activation of lysosomal function during dendritic cell maturation. *Science* **2003**, *299* (5611), 1400–3. (c) Kogot-Levin, A.; Zeigler, M.;

- Ornoy, A.; Bach, G. Mucopolipidosis type IV: the effect of increased lysosomal pH on the abnormal lysosomal storage. *Pediatr. Res.* **2009**, *65* (6), 686–90. (d) Colacurcio, D. J.; Nixon, R. A. Disorders of lysosomal acidification-The emerging role of v-ATPase in aging and neurodegenerative disease. *Ageing Res. Rev.* **2016**, *32*, 75–88. (e) Yu, M.; Wu, X.; Lin, B.; Han, J.; Yang, L.; Han, S. Lysosomal pH Decrease in Inflammatory Cells Used To Enable Activatable Imaging of Inflammation with a Sialic Acid Conjugated Profluorophore. *Anal. Chem.* **2015**, *87* (13), 6688–95.
- (3) (a) Wu, S.; Li, Z.; Han, J.; Han, S. Dual colored mesoporous silica nanoparticles with pH activable rhodamine-lactam for ratiometric sensing of lysosomal acidity. *Chem. Commun.* **2011**, *47* (40), 11276–8. (b) Marín, M.; Galindo, F.; Thomas, P.; Russell, D. Localized Intracellular pH Measurement Using a Ratiometric Photoinduced Electron-Transfer-Based Nanosensor. *Angew. Chem.* **2012**, *124*, 9795–9799. (c) Chiu, Y. L.; Chen, S. A.; Chen, J. H.; Chen, K. J.; Chen, H. L.; Sung, H. W. A dual-emission Förster Resonance Energy Transfer nanoprobe for sensing/imaging pH changes in biological environment. *ACS Nano* **2010**, *4*, 7467–7474. (d) Pan, W.; Wang, H.; Yang, L.; Yu, Z.; Li, N.; Tang, B. Ratiometric Fluorescence Nanoprobes for Subcellular pH Imaging with a Single-Wavelength Excitation in Living Cells. *Anal. Chem.* **2016**, *88*, 6743–6748. (e) Chan, Y.; Wu, C.; Ye, F.; Jin, Y.; Smith, P.; Chiu, D. Development of Ultrabright Semiconducting Polymer Dots for Ratiometric pH Sensing. *Anal. Chem.* **2011**, *83*, 1448–1455. (f) Peng, H. S.; Stolwijk, J. A.; Sun, L. N.; Wegener, J.; Wolfbeis, O. S. A Nanogel for Ratiometric Fluorescent Sensing of Intracellular pH Values. *Angew. Chem.* **2010**, *122*, 4342–4345. (g) Shi, W.; Li, X.; Ma, H. A Tunable Ratiometric pH Sensor Based on Carbon Nanodots for the Quantitative Measurement of the Intracellular pH of Whole Cells. *Angew. Chem.* **2012**, *124*, 6538–6541.
- (4) (a) Wan, Q.; Chen, S.; Shi, W.; Li, L.; Ma, H. Lysosomal pH rise during heat shock monitored by a lysosome-targeting near-infrared ratiometric fluorescent probe. *Angew. Chem., Int. Ed.* **2014**, *53* (41), 10916–20. (b) Li, G.; Zhu, D.; Xue, L.; Jiang, H. Quinoline-based fluorescent probe for ratiometric detection of lysosomal pH. *Org. Lett.* **2013**, *15* (19), 5020–3. (c) Kim, H. J.; Heo, C. H.; Kim, H. M. Benzimidazole-based ratiometric two-photon fluorescent probes for acidic pH in live cells and tissues. *J. Am. Chem. Soc.* **2013**, *135* (47), 17969–77.
- (5) (a) Dong, B.; Song, X.; Wang, C.; Kong, X.; Tang, Y.; Lin, W. Dual Site-Controlled and Lysosome-Targeted Intramolecular Charge Transfer-Photoinduced Electron Transfer-Fluorescence Resonance Energy Transfer Fluorescent Probe for Monitoring pH Changes in Living Cells. *Anal. Chem.* **2016**, *88*, 4085–4091. (b) Li, Z.; Wu, S.; Han, J.; Yang, L.; Han, S. Resolution of lysosomes in living cells with a ratiometric molecular pH-meter. *Talanta* **2013**, *114*, 254–60. (c) Song, G. J.; Bai, S. Y.; Luo, J.; Cao, X. Q.; Zhao, B. X. A Novel Water-soluble Ratiometric Fluorescent Probe Based on FRET for Sensing Lysosomal pH. *J. Fluoresc.* **2016**, *26* (6), 2079–2086. (d) Wang, Q.; Zhou, L.; Qiu, L.; Lu, D.; Wu, Y.; Zhang, X. B. An efficient ratiometric fluorescent probe for tracking dynamic changes in lysosomal pH. *Analyst* **2015**, *140* (16), 5563–9. (e) Zhang, X. Z.; Zhang, T.; Shen, S.; Miao, J.; Zhao, B. A ratiometric lysosomal pH probe based on the naphthalimide–rhodamine system. *J. Mater. Chem. B* **2015**, *3*, 3260–3266.
- (6) Xue, Z.; Zhao, H.; Liu, J.; Han, J.; Han, S. Responsive hetero-organellar partition conferred fluorogenic sensing of mitochondrial depolarization. *Chem. Sci.* **2017**, DOI: 10.1039/C6SC04158B.
- (7) Li, C.; Evans, R. M. Ligation independent cloning irrespective of restriction site compatibility. *Nucleic Acids Res.* **1997**, *25* (20), 4165–6.
- (8) (a) Hasegawa, T.; Kondo, Y.; Koizumi, Y.; Sugiyama, T.; Takeda, A.; Ito, S.; Hamada, F. A highly sensitive probe detecting low pH area of HeLa cells based on rhodamine B modified beta-cyclodextrins. *Bioorg. Med. Chem.* **2009**, *17* (16), 6015–9. (b) Wu, X.; Yu, M.; Lin, B.; Xing, H.; Han, J.; Han, S. A sialic acid-targeted near-infrared theranostic for signal activation based intraoperative tumor ablation. *Chem. Sci.* **2015**, *6*, 798–603. (c) Zhang, W.; Tang, B.; Liu, X.; Liu, Y.; Xu, K.; Ma, J.; Tong, L.; Yang, G. A highly sensitive acidic pH fluorescent probe and its application to HepG2 cells. *Analyst* **2009**, *134* (2), 367–71.
- (9) Tian, Y.; Yu, M.; Li, Z.; Han, J.; Yang, L.; Han, S. Optical tracking of phagocytosis with an activatable profluorophore metabolically incorporated into bacterial peptidoglycan. *Anal. Chem.* **2015**, *87* (16), 8381–6.
- (10) Kang, J. S.; Kostov, Y. Ratiometric pH measurements using LysoSensor DND-192. *J. Biochem. Mol. Biol.* **2002**, *35* (4), 384–8.
- (11) Yoshimori, T.; Yamamoto, A.; Moriyama, Y.; Futai, M.; Tashiro, Y. Bafilomycin A1, a specific inhibitor of vacuolar-type H(+)-ATPase, inhibits acidification and protein degradation in lysosomes of cultured cells. *J. Biol. Chem.* **1991**, *266* (26), 17707–12.
- (12) (a) Deretic, V.; Saitoh, T.; Akira, S. Autophagy in infection, inflammation and immunity. *Nat. Rev. Immunol.* **2013**, *13* (10), 722–37. (b) Irrcher, I.; Park, D. S. Parkinson's disease: to live or die by autophagy. *Sci. Signaling* **2009**, *2* (65), pe21.
- (13) Fleming, A.; Noda, T.; Yoshimori, T.; Rubinsztein, D. C. Chemical modulators of autophagy as biological probes and potential therapeutics. *Nat. Chem. Biol.* **2011**, *7*, 9–17.
- (14) Chikte, S.; Panchal, N.; Warnes, G. Use of LysoTracker dyes: A flow cytometric study of autophagy. *Cytometry, Part A* **2014**, *85*, 169–178.
- (15) Vanden Berghe, T.; Linkermann, A.; Jouan-Lanhouet, S.; Walczak, H.; Vandenabeele, P. Regulated necrosis: the expanding network of non-apoptotic cell death pathways. *Nat. Rev. Mol. Cell Biol.* **2014**, *15*, 135–47.
- (16) Liu, X.; Kim, C.; Yang, J.; Jemerson, R.; Wang, X. Induction of apoptotic program in cell-free extracts: requirement for dATP and cytochrome c. *Cell* **1996**, *86*, 147–157.
- (17) Deshmukh, M.; Johnson, E. M., Jr. Staurosporine-induced neuronal death: multiple mechanisms and methodological implications. *Cell Death Differ.* **2000**, *7* (3), 250–61.
- (18) Superti, F.; Seganti, L.; Ruggeri, F. M.; Tinari, A.; Donelli, G.; Orsi, N. Entry pathway of vesicular stomatitis virus into different host cells. *J. Gen. Virol.* **1987**, *68*, 387–99.
- (19) Akhtar, J.; Shukla, D. Viral entry mechanisms: cellular and viral mediators of herpes simplex virus entry. *FEBS J.* **2009**, *276* (24), 7228–36.
- (20) (a) Nicola, A. V.; Hou, J.; Major, E. O.; Straus, S. E. Herpes simplex virus type 1 enters human epidermal keratinocytes, but not neurons, via a pH-dependent endocytic pathway. *J. Virol.* **2005**, *79* (12), 7609–16. (b) Nicola, A. V.; McEvoy, A. M.; Straus, S. E. Roles for endocytosis and low pH in herpes simplex virus entry into HeLa and Chinese hamster ovary cells. *J. Virol.* **2003**, *77* (9), 5324–32.